Frequency dependence and equilibration of the specific heat of glass-forming liquids

Clare C. Yu and Hervé M. Carruzzo*
Department of Physics and Astronomy, University of California, Irvine, California 92697, USA
(Received 20 August 2002; published 21 May 2004)

We have performed molecular dynamics simulations on a glass-forming liquid consisting of a three-dimensional binary mixture of soft spheres. We show that a peak in the specific heat versus temperature can occur because a glassy system that shows no signs of aging progresses so slowly through the energy landscape that the minimum sampling time needed to obtain accurate thermodynamic averages exceeds the observation time. We develop a systematic technique to determine the equilibrium value of the specific heat and the minimum sampling time. Below the temperature of the specific heat peak, the minimum sampling time is orders of magnitude longer than the α relaxation time. We find that an equilibrium system that is not undergoing structural relaxation or aging has a frequency dependent specific heat that rises as the frequency decreases. The rise occurs at frequencies corresponding to periods that are long enough for the system to sample statistically independent energies. When the period is comparable to the minimum sampling time, the frequency dependent specific heat reaches a plateau. As a result, the specific heat has a frequency dependence at frequencies orders of magnitude lower than is implied by the inverse α relaxation time.

DOI: 10.1103/PhysRevE.69.051201 PACS number(s): 65.20.+w, 64.70.Pf, 02.70.Ns, 05.20.−y

I. INTRODUCTION

As a glass-forming liquid is cooled, a glass transition occurs when the system falls out of equilibrium, i.e., when the time scale for reaching equilibrium exceeds the observation time [1]. This is often associated with frequency dependent measurements of quantities such as the specific heat [2] and dielectric function [3] where characteristic frequencies systematically decrease with decreasing temperature even when the samples show no signs of aging. In this paper we show that this frequency dependence is associated with long equilibration times.

Like many complex systems, such as proteins and neural networks, the dynamics of the glass transition is governed by the potential energy landscape where each point corresponds to a particular configuration and energy of the system [4,5]. The energy landscape can be used to describe the three ways in which a system can fall out of equilibrium. First a system can become trapped in a metastable minimum where it stays for the duration of the observation time. Second a system can be in an energetically unlikely part of phase space and proceed slowly to a region where its configurations obey a Boltzmann distribution. As such a nonequilibrium system evolves toward more probable regions of phase space, it exhibits aging which means its properties systematically change with time and do not obey stationarity [6]. The aging time, after which aging stops, is equal to the α relaxation time which is the charactistic time for the system to forget its initial configuration.

The third way to fall out of equilibrium is to inadequately sample an equilibrium ensemble. It is often not appreciated just how long it actually can take to acquire enough values, and how this time is related to the frequency dependence in measured quantities. The point is that even after a glassy system no longer ages and has reached basins with appropriate energies, the system proceeds so slowly through the energy landscape that the α relaxation time is easily dwarfed by the minimum sampling time which we define as the time to accumulate the large number of statistically independent measurements needed to accurately determine a thermodynamic average. We find from molecular dynamics simulations that a glass-forming liquid, that shows no signs of aging, can undergo a glass transition, as signaled by a peak in the specific heat C_V versus temperature, when the observation time drops below the minimum sampling time. The distribution of energies that a system samples in a basin of the energy landscape is a subset of the full distribution of energies available to the system. Since this subset has a smaller variance than the full distribution, the resulting specific heat, which is proportional to the variance of the energy, will be smaller when calculated from short time spans than from long time spans. These smaller values account for the values below the peak in C_V on the low temperature side. Going to longer time spans eliminates the peak, though at temperatures below the peak temperature T_p, these time spans can be orders of magnitude longer than previously recognized equilibration times such as the α relaxation time, the energy correlation time, and the aging time.

Several groups [7,8] have claimed to find equilibrium peaks in the specific heat in their simulations of glass forming liquids. However, their criterion for deciding if they had equilibrium values of the specific heat were somewhat arbitrary. They believed that their systems were in equilibrium because they had run longer than the α relaxation time, but they had no definitive way of testing this. In this paper we present a systematic method to determine the equilibrium value of the specific heat. This technique tracks the value of the specific heat as a function of the measurement time span. When the specific heat stops increasing and saturates with increasing time span, C_V has reached its equilibrium value. We use this procedure to eliminate the peak in the specific heat that we found using parallel tempering simulations.

*Present address: Internap, Atlanta, GA 30309.

One way to probe the time scales involved in glassy systems is via the frequency dependence of the specific heat. Experimental measurements on equilibrium systems find that as the frequency decreases, the real part of the specific heat rises in a characteristic frequency range before reaching a plateau [2,3,9–15]. The characteristic frequency decreases as the temperature decreases. These experiments have inspired a number of theoretical approaches [16–25]. Some have derived an expression for the frequency dependent specific heat within an existing theoretical framework such as generalized hydrodynamics [17,18,23], the fluctuation-dissipation theorem [22], projection operator formalism [25], or generalized constitutive equations [21]. Simulations have been able to reproduce the same qualitative features that are seen experimentally [19,25]. Some papers attribute the increase in the specific heat at low frequencies (as the frequency decreases) to the structural relaxation of the supercooled liquid since both the characteristic frequency and the relaxation time increase with decreasing temperature [18,23]. Scheidler *et al.* [25] note from their simulations that the specific heat increase occurs at frequencies which have periods corresponding to the time scales of the structural relaxation. Others have proposed that the measurement technique forces the system out of equilibrium when the structural relaxation time is longer than the inverse frequency of the applied heat current oscillations [16]. We show from our simulations that in a system that is no longer aging, structural relaxation is not directly responsible for the specific heat behavior at low frequencies because the system is already in equilibrium and does not need to relax to an equilibrium configuration. Rather the increase of the frequency dependent specific heat with decreasing frequency mirrors the increase of the specific heat with time span because longer time spans correspond to longer periods and lower frequencies. During a period the system is exploring the energy landscape. The longer the period, the more statistically independent energies it can sample. When the period is long enough for the system to sample statistically independent energies, the specific heat rises. We find that the energy correlation time, which is comparable to the α relaxation time, determines the characteristic frequency range where the specific heat rises. The fact that the minimum sampling time exceeds the α relaxation time and the energy correlation time by orders of magnitude implies that the specific heat should increase down to frequencies much lower than the inverse α relaxation time. This is indeed the case, and we find that the frequency dependent specific heat saturates at a frequency corresponding to the inverse of the minimum sampling time.

The paper is organized as follows. In Sec. II we describe the details of our molecular dynamics simulations including parallel tempering and single temperature runs. We also describe our calculation of the α relaxation time. In Sec. III A we show that parallel tempering calculations produce a peak in the specific heat versus temperature. In Sec. III A 1 we show by plotting the inherent structure energies versus temperature that the specific heat peak is not the result of getting stuck in a basin of the energy landscape. We present in Sec. III B a systematic method to determine the equilibrium value of the specific heat. This technique tracks the value of the specific heat as a function of the measurement time span. We use it to show that the specific heat peak is eliminated when equilibrium values are used. In Sec. III B 1 we give a functional fit to the equilibrium specific heat. In Sec. III B 2 we discuss the energy correlation time and explain why the specific heat increases with increasing time span until it reaches its equilibrium value. In Sec. III C we show that the frequency dependence of the specific heat mirrors the increase of the specific heat with time span. In Sec. III D we show that the increase of the specific heat with time span occurs in systems which are not aging. We also show that even when the root mean square displacement is comparable to the size of the system, the system still has not sampled enough configurations to obtain its thermodynamic value. In Sec. IV we present our explanation of the frequency dependent specific heat and discuss our results.

II. MOLECULAR DYNAMICS SIMULATION

We have performed a molecular dynamics simulation on a three-dimensional glass forming liquid [26,27] consisting of a 50:50 mixture of two sizes of soft spheres, labeled A and B. The interaction between two particles a distance r apart is given by $V_{\alpha\beta}(r)=\epsilon[(\sigma_{\alpha\beta}/r)^{12}+X_{\alpha\beta}(r)]$ where the interaction length $\sigma_{\alpha\beta}=(\sigma_\alpha+\sigma_\beta)/2$, and the ratio of the diameters $\sigma_B/\sigma_A=1.4(\alpha,\beta=A,B)$. The cutoff function $X_{\alpha\beta}(r)=r/\sigma_{\alpha\beta}-\lambda$ with $\lambda=13/12^{12/13}$. The interaction is cutoff at the minimum of the potential $V_{\alpha\beta}(r)$ where the potential and its first derivative $V'_{\alpha\beta}(r)$ with respect to r are equal to zero. This cutoff ensures that $V_{\alpha\beta}(r)$ and $V'_{\alpha\beta}(r)$ go smoothly to zero. Energy and length are measured in units of ϵ and σ_A, respectively. Temperature is in units of ϵ/k_B, and time is in units of $\sigma_A\sqrt{m/\epsilon}$ where the unit of mass m is the mass of the particles ($m_A=m_B=m$). We will refer to these units as MD (molecular dynamics) units. During each run the density $\rho_0=N/L^3=0.6$ was fixed. $N=N_A+N_B$ is the total number of particles. The system occupies a cube of volume L^3 with periodic boundary conditions. According to the ideal mode coupling theory [28], the relaxation time diverges at a temperature T_C. For our system $T_C=0.303$ [29].

The equations of motion were integrated using the leap-frog method [30] with a time step of 0.005. We keep the temperature constant using an algorithm [30] that introduces a nonholonomic constraint into the equations of motion in order to fix the kinetic energy [31,32], rather than fixing the total energy. The justification for this is based on a formulation of mechanics known as Gauss' principle of least constraint [33], which states that $\Sigma_i m_i(\ddot{\vec{r}}_i-\vec{F}_i/m_i)^2$ is minimized by the constrained motion. The constraint means that the motion is non-Newtonian, but this is fine since we are concerned with thermodynamics rather than dynamics. We require that the temperature remain fixed to an accuracy of 5×10^{-4}. We monitored the temperature and found that the temperature constraint algorithm worked so well that once the temperature was set, the program rarely had to rescale the velocities in order to adjust the temperature. Since temperature rather than energy is kept constant, it can be shown that we are working in the canonical ensemble [34].

We have done three types of runs in our molecular dynamics simulations: cooling, parallel tempering, and single

temperature runs. First we describe our cooling runs. We cool the system from a high temperature ($T=1.5$) by lowering the temperature in steps of $\Delta T=0.05$. At each temperature we equilibrate for 10^4 time steps and then measure the quantities of interest for 10^7 additional steps. The results are then averaged over different runs.

At the glass transition the system falls out of equilibrium and becomes trapped in a basin of the energy landscape. In order to try to avoid this, we have used parallel tempering together with molecular dynamics. We implement parallel tempering (PT) [29,35] by running molecular dynamics simulations in parallel at chosen temperatures using the temperature constraint algorithm [30] to keep the temperature of each simulation constant. At 100 time step intervals we attempt to switch the configurations of two neighboring temperatures using a Metropolis test which ensures that the energies of the configurations sampled at any given temperature have a Boltzmann distribution. Let β_1 and β_2 be two neighboring inverse temperatures, and let U_1 and U_2 be the corresponding potential energies of the configurations at these temperatures at a time step just before the possible swap. If $\Delta=(\beta_1-\beta_2)(U_2-U_1)$, then the switch is accepted with probability unity if $\Delta\leqslant 0$ and with probability $\exp(-\Delta)$ if $\Delta>0$. The acceptance ratio is between 30% and 75%. Near T_p, the acceptance ratio was above 60%. After a swap is accepted, the velocities of the particles in each configuration are rescaled to suit their new temperature. Each configuration then continues to evolve using molecular dynamics for another 100 time steps. Switching configurations allows a given simulation to do a random walk in temperature space in which it visits both low temperatures and high temperatures. This helps to prevent it from becoming trapped in a valley of the energy landscape at low temperatures. Typically we equilibrate for 2×10^6 time steps and then do measurements for an additional $(4-10)\times10^6$ MD steps. We average over different runs which have different initial positions and velocities of the particles at each temperature.

We have also done some long runs at a single temperature by starting from a configuration generated by parallel tempering, equilibrating for up to 5×10^7 time steps, and then making measurements for 10^8 time steps. The usefulness of these runs will become clear later.

To set the time scale, we have calculated the α relaxation time using the full intermediate scattering function $F_{BB}(\vec{k},t)=(1/N_B)\langle\rho_{\vec{k}}(t)\rho_{-\vec{k}}(0)\rangle$ for the B particles where N_B is the number of B particles and $\rho_{\vec{k}}(t)=\Sigma_{i=1}^{N_B}\exp[-i\vec{k}\cdot\vec{r}_i(t)]$ is the Fourier transform of the density at time t. $\langle\ldots\rangle$ denotes the thermal average. Since the system is isotropic, we choose the wave vectors whose magnitude equals $k_{\max}$ which is the wave vector of the maximum in the partial static structure factor $S_{BB}(k)$ for the B particles, because $F_{BB}(k,t)$ relaxes slowest at $k_{\max}$ [36]. The relaxation time τ is defined by $F(k,\tau)/F(k,t=0)=1/e$ [37,38]. We have averaged $F(k,t)/F(k,t=0)$ over 40 runs after waiting times of 5×10^7, 10^8, and 1.5×10^8 time steps for a system with 512 particles at $T=0.289\,855$ which is slightly below T_p and T_C [29]. We find that the α relaxation time $\tau=(1.0\pm0.1)\times10^6$ MD time steps. This gives us a time scale by which to compare other times such as our run times. This value of τ shows no signs of aging [6] in the sense that there is no systematic variation with waiting time. The fluctuations in τ for the three different waiting times is indicated by the cited standard deviation. At higher temperatures this relaxation time is much shorter [29].

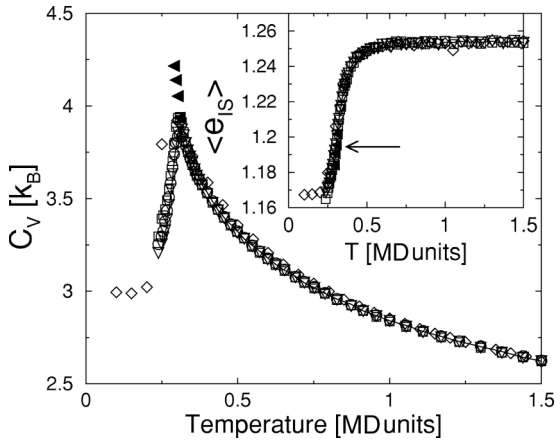

FIG. 1. Specific heat vs temperature. Shown is the specific heat calculated from fluctuations for systems with $N=216$ (○, averaged over six runs) and with $N=512$ for measurements covering 4×10^6 time steps (▽, averaged over nine runs) and 10^7 time steps (□, averaged over three runs) done with parallel tempering. Typical equilibration times were 2×10^6 time steps. The solid line is the specific heat calculated from the derivative of the energy from the 4×10^6 time step parallel tempering runs with $N=512$. Also shown is the specific heat calculated from the energy fluctuations for a system with $N=512$ (◇, averaged over six runs) that was cooled conventionally with 10^7 time steps per temperature. The ◀ correspond to concatenating between 13 and 40 single temperature runs; each run had 10^8 time steps with 512 particles that were initiated from parallel tempering configurations and equilibrated for up to 5×10^7 time steps. Inset: Average inherent structure energy per particle vs. temperature for 512 particles obtained from parallel tempering, cooling, and single temperature runs. The symbols denote the same cases as in the main figure. The arrow points to the inflection point that coincides with T_p. $\langle e_{IS}\rangle$ is measured in MD units.

III. RESULTS

A. Specific heat

We calculate the specific heat C_V per particle at constant volume V in two ways. The first uses the fluctuations in the potential energy U per particle: $C_V=(3k_B/2)+Nk_B\beta^2(\langle U\rangle^2-\langle U\rangle^2)$ where the first term is the kinetic energy. The second way uses $C_V=(3k_B/2)+d\langle U\rangle/dT\approx(3k_B/2)+(\langle U(T_{i+1})\rangle-\langle U(T_i)\rangle)/(T_{i+1}-T_i)$ where we approximate the derivative with a finite difference between neighboring temperatures. The results are shown in Fig. 1. Note that there is a sharp asymmetric peak centered at $T_p=0.305\pm0.003$. The low temperature side of the peak drops steeply. The curves for 216 and 512 particles coincide, indicating that there is no size dependence. The discrete points are calculated from the energy fluctuations. The solid line is calculated from the derivative of the energy. The fact that the two coincide indicates that the system was equilibrated in all the basins of the

energy landscape that were visited. For comparison we also show the result of cooling through the transition ($\diamond$). The peak in C_V found by cooling coincides with the peak found in parallel tempering.

1. Inherent structure energies

We do not believe that the parallel tempering peak in the specific heat is due to the system becoming trapped in a metastable minimum in the energy landscape for the following reason. The configurations corresponding to the minima of the energy landscape are called inherent structures [39]. We sampled the configurations that were visited during the parallel tempering runs and found the corresponding inherent structure energy e_{IS} per particle by minimizing the potential energy locally using the method of conjugate gradients [40]. In the inset of Fig. 1 we plot the average inherent structure energies versus the temperature of the configuration that was originally saved. At high temperatures ($T \gtrsim 0.5$) $\langle e_{IS} \rangle$ does not vary much with temperature. As the temperature decreases below 0.5, $\langle e_{IS} \rangle$ decreases rather steeply [5]. The temperature of the inflection point of this decrease coincides with the temperature T_p of the peak in the specific heat. We also show $\langle e_{IS} \rangle$ for a system of 512 particles that was cooled from $T=1.5$. At low temperatures $\langle e_{IS} \rangle$ is rather independent of temperature for the cooled system, indicating that the system is trapped in an energy basin. Such a flattening off with decreasing temperature is not observed when parallel tempering is used, indicating that the system is able to continue visiting deeper basins.

B. Specific heat dependence on measurement time span

The plot of $\langle e_{IS} \rangle$ versus T indicates that the system does not appear to be trapped in a valley of the energy landscape at $T \lesssim T_p$. However, the peak in the specific heat is not an equilibrium feature. Rather it is the result of not sampling enough of phase space below T_p. None of the runs we have shown at $T < T_p$ have reached the minimum sampling time. In order to obtain an accurate thermodynamic average, we have developed a method which we now describe. We did single temperature runs in which we took a configuration of 512 particles generated by parallel tempering at $T = 0.289\,855$, equilibrated for 5×10^7 time steps, and then ran for an additional 10^8 time steps during which we recorded the energy at every time step. Then we did block averaging in which we divided our 1×10^8 time steps into equal segments, each of length Δt_b, and calculated the specific heat from energy fluctuations for each segment [41]. The block averaged specific heat versus time for two different time spans Δt_b is shown in the inset of Fig. 2. Note that for any given time span, there is no sign of systematic aging. However, the specific heat averaged over time increases with Δt_b.

The specific heat, averaged over time spans of a given size and over different runs, versus time span size Δt_b at several temperatures is shown in Fig. 2 by the solid lines. To obtain time spans that are longer than any given run, we concatenated the energies from the runs done at a given temperature to make one huge run, and then did block averaging

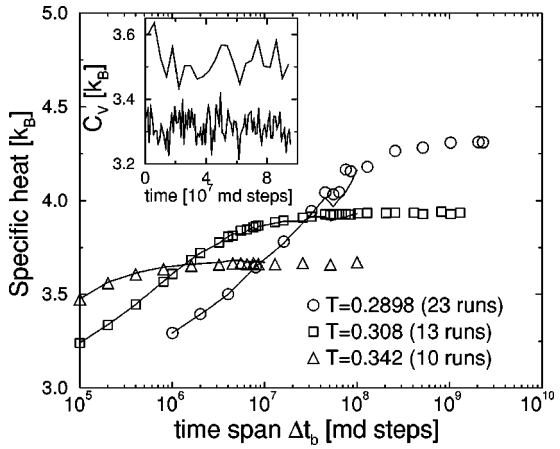

FIG. 2. Block averaged specific heat vs time span Δt_b for 512 particles at $T = 0.289\,855$, 0.308 642, and 0.342 4658. Solid lines are the result of block averaging each run and then averaging over the number of runs shown. Open symbols are the result of stringing runs together and then block averaging. The shape of the symbols indicates the temperature as given in the legend. Inset: Block averaged specific heat vs time for 512 particles at $T = 0.289\,855$. The lower curve corresponds to $\Delta t_b = 10^6$ MD steps, and the upper to $\Delta t_b = 4 \times 10^6$ MD steps. The time is the time (in units of 10^7 MD steps) in the middle of each block. The data at $T = 0.289\,855$ is averaged over 23 runs. Parameters for both figures are the same as in Fig. 1.

on the huge run. We call this global averaging. The results are shown as open symbols in Fig. 2. There is good agreement between the solid lines and open symbols. Note that the specific heat initially increases with time span but then levels off when the time span is long enough to exceed the minimum sampling time. This time increases with decreasing temperature. Thus at $T = 0.289\,855 < T_p$, the specific heat continues to increase with time span up to $\Delta t_b = 2 \times 10^8$ time steps which is 200 times longer than the α relaxation time τ. Equilibrated values of C_V near T_p are plotted in Fig. 1 and 3 and lie above the peak in C_V found with parallel tempering. Thus the specific heat peak found with parallel tempering is the result of not sampling enough of phase space at $T < T_p$ to obtain the true thermodynamic value of the specific heat C_V^{true}. The exploration of the energy distribution below T_p is slow even with parallel tempering because the probability of sampling large increases in U are exponentially small.

1. Temperature dependence of the specific heat

As Fig. 3 shows, the equilibrium specific heat continues to rise with decreasing temperature down to $T = 0.2898$. In the temperature range shown, the specific heat can be fitted to the form $C_V = A_1 T^{B_1} + A_2 T^{B_2}$, where $A_1 = 2.845 k_B$, $B_1 = -0.20986$, $A_2 = 3.477 \times 10^{-4} k_B$, and $B_2 = -5.804$. The first term dominates at high temperatures ($T > 0.57$) where $C_{V,hiT} \sim T^{-0.21}$. In this temperature range the specific heat for the binary mixture coincides with that of the single component fluid that has $\sigma = \sigma_A$, a density of 1.1 and crystallizes at a melting temperature $T_m = 0.57$. At lower temperatures the specific heat rises steeply and the second term that goes as $\sim T^{-5.8}$ comes into play. Since $C_V/T = dS/dT|_V$, the steep rise

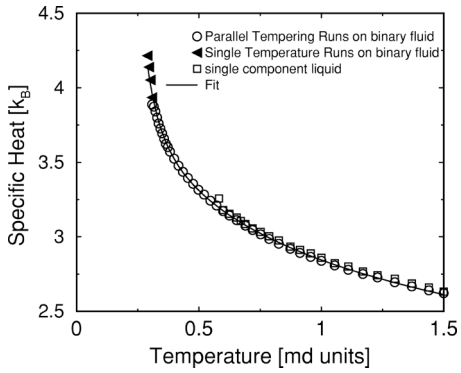

FIG. 3. Equilibrium specific heat vs temperature. Shown is the specific heat calculated from fluctuations for systems with $N=512$ (○, averaged over nine runs) for measurements covering 4×10^6 time steps done with parallel tempering. Typical equilibration times were 2×10^6 time steps. The ◀ come from global averaging as shown in Fig. 2, i.e., from concatenating between 13 and 40 single temperature runs; each run had 10^8 time steps with 512 particles that were initiated from parallel tempering configurations and equilibrated for up to 5×10^7 time steps. Parameters are the same as in Fig. 1. The □ symbols represent the specific heat calculated from the energy fluctuations of a single component fluid ($N=512$, $\sigma=\sigma_A$, $\rho=1.1$) that crystallizes at a melting temperature $T_m=0.565$. The single component fluid specific heat was averaged over three parallel tempering runs that were equilibrated for 1×10^6 time steps and then run for an additional 2×10^6 time steps at each temperature. The solid line is a fit to the form $C_V=A_1T^{B_1}+A_2T^{B_2}$, where $A_1=2.845k_B$, $B_1=-0.209\,86$, $A_2=3.477\times10^{-4}k_B$, and $B_2=-5.804$.

in the specific heat means that the entropy versus temperature has a steep positive slope. Since the crystalline entropy has a shallower slope, this is consistent with the Kauzmann paradox in which the low temperature extrapolation of the entropy of the glass intersects the crystalline entropy. This raises the very interesting question of what happens to the specific heat in the thermodynamic limit as the temperature falls. Does the specific heat continue to rise? Does it eventually go through a peak? Unfortunately the answers lie at temperatures where we cannot find the equilibrium value in a reasonable amount of time.

2. Energy correlation time and energy distribution

Note that C_V^{true} is proportional to the variance σ_U^2 of the potential energy distribution $P(U)$, i.e., $C_V^{\text{true}}=N\sigma_U^2/(k_BT^2)$. If σ_U^2 is finite and if n sample values of U are statistically independent and identically distributed, then basic statistics dictates that the measured C_V, which is proportional to the sample variance S_n^2 of U, has an expectation value of $\langle C_V\rangle=C_V^{\text{true}}(1-1/n)$ [41]. The number n of statistically independent potential energies is given by $n=\Delta t_b/\tau_U$ where τ_U is the energy correlation time. Fitting the data that is within 5% to 10% of C_V^{true} in Fig. 2 to $\langle C_V\rangle=C_V^{\text{true}}(1-1/n)$ yields $\tau_U\approx3\times10^6$, 1×10^5, and 5×10^3 time steps at $T=0.289\,855\,1$, 0.308 642, and 0.342 466, respectively. These values are comparable to the α relaxation times τ of 1×10^6, 6×10^4, and 2×10^4 time steps, respectively.

They are also comparable to the correlation time given by the statistical inefficiency s [42]. s is the $\Delta t_b\to\infty$ limit of the product of Δt_b and the ratio of the variance of the average block energies to the variance of the energies:

$$s=\lim_{\Delta t_b\to\infty}\frac{\Delta t_b\sigma^2(\overline{U}_b)}{\sigma^2(U)}, \tag{1}$$

where the variance of the energies is $\sigma^2(U)=(\Delta t_{\text{run}})^{-1}\Sigma_{t=1}^{\Delta t_{\text{run}}}(U(t)-\overline{U}_{\text{run}})^2$, the variance of the average block energies is $\sigma^2(\overline{U}_b)=n_b^{-1}\Sigma_{b=1}^{n_b}(\overline{U}_b-\overline{U}_{\text{run}})^2$, the average block energy is $\overline{U}_b=(\Delta t_b)^{-1}\Sigma_{t=1}^{\Delta t_b}U(t)$, the average energy is $\overline{U}_{\text{run}}=(\Delta t_{\text{run}})^{-1}\Sigma_{t=1}^{\Delta t_{\text{run}}}U(t)$, and the number of blocks $n_b=\Delta t_{\text{run}}/\Delta t_b$. To find s, we calculate the ratio $\Delta t_b\sigma^2(\overline{U}_b)/\sigma^2(U)$ for each run for various time spans Δt_b. Then for each time span we average the ratio over all the runs at a given temperature. By plotting the ratio versus Δt_b^{-1} on a log–log plot, we can extrapolate $(\Delta t_b)^{-1}$ to 0 to estimate s. We expect $s\approx2\tau_U$, and we find that $s/2$ is comparable to τ_U and τ. $s\approx2.4\times10^6$, 2.5×10^5, and 1.1×10^4 time steps at $T=0.289\,855$, 0.308642, and 0.342466, respectively. Figure 4 shows that the α relaxation time and the energy correlation time $\tau_\varepsilon\equiv s/2$ are quite comparable at various temperatures. These values of τ_U and τ_ε imply that the energies are correlated over quite a number of time steps, and that the number n of statistically independent values is substantially smaller than the total number of energies.

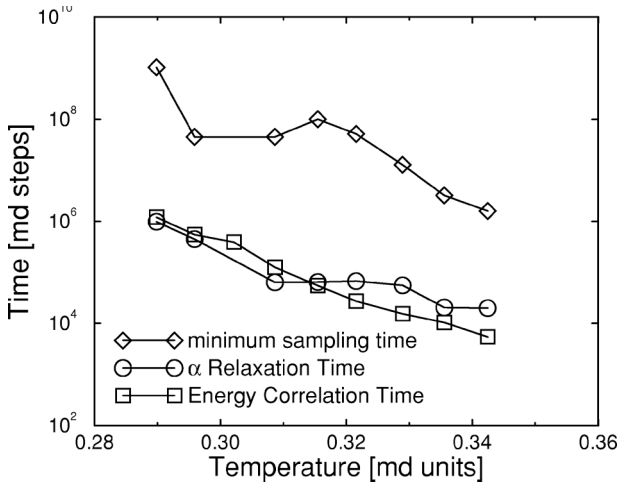

FIG. 4. Minimum sampling time, α relaxation time τ, and the energy correlation time τ_ε which is half of the statistical inefficiency as a function of temperature. Note that all have roughly the same temperature dependence. Note also that τ and τ_ε are comparable.

We find that $\langle C_V\rangle$ is a good fit to $\langle C_V\rangle=C_V^{\text{true}}(1-1/n)$ only when $\langle C_V\rangle$ is within 5% to 10% of C_V^{true}. At shorter time spans and lower temperatures Fig. 2 shows that $C_V\sim\ln(\Delta t_b)$. This occurs because the system does not uniformly sample $P(U)$ during these shorter time spans. As the system travels through the energy landscape, it samples the energies of each basin that it visits. As shown in Fig. 5, we find that the distribution of energies sampled from the basins visited during a shorter time span has a smaller variance than the total distribution $P(U)$. Furthermore, the centers of the

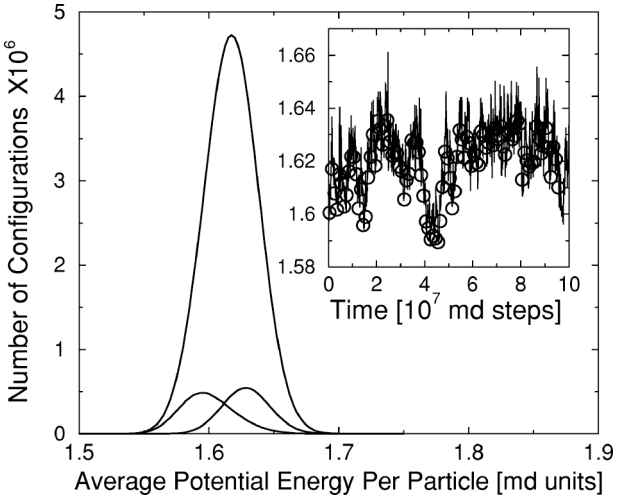

FIG. 5. Number of configurations vs the average energy per particle acquired during one run of 10^8 MD steps of a system of 512 particles at $T=0.289\,855$. The large curve centered at 1.62 is the histogram for the entire run. The small curve on the left centered at 1.60 represents the counts acquired between 4×10^7 and 5×10^7 time steps; the small curve on the right centered at 1.63 represents the counts acquired between 7×10^7 and 8×10^7 time steps. Inset: Data from the same run. Circles represent the potential energy per particle averaged over 10^6 time steps vs time. The solid line is $e_{IS}+3k_BT/2$ vs time. The potential energy per particle is measured in MD units.

smaller distributions do not necessarily coincide with the center of the total distribution. Rather the smaller distributions are centered at the inherent structure energy plus the energy of vibrations around e_{IS} [43]. In support of this, we show in the inset of Fig. 5 that the block averaged energy versus time approximately coincides with $[e_{IS}(t)+3k_BT/2]$ versus time. As more basins are visited, the sample average $\langle U\rangle$ moves towards the average of the full distribution and the variance grows. This corresponds to C_V increasing with time span since C_V is proportional to the variance of the potential energy distribution.

C. Frequency dependent specific heat

The increase of the specific heat with time span is mirrored in the frequency dependence of the specific heat because lower frequencies correspond to longer periods and longer time spans. To show this, we have calculated the real part of the frequency dependent specific heat which is given by [19,22]

$$C_V'(\omega) = (3k_B/2) + \phi_V(t=0) - \omega\int_0^\infty \phi_V(t)\sin(\omega t)dt, \quad (2)$$

where the energy autocorrelation function $\phi_V(t) = Nk_B\beta^2\langle(U(t)-\langle U\rangle)(U(0)-\langle U\rangle\rangle_{t_0}$ and $\langle\ldots\rangle_{t_0}$ indicates an average over initial times. The subscript V means that the volume is kept constant. Since the time to calculate $\phi_V(t)$ goes with the number of energies squared, we used energies recorded at intervals of 350 MD steps. The exclusion of short times reduces the value of $C_V(\omega)$ and gives the Fourier sine integral a nonzero lower limit which introduces oscillations into $C_V(\omega)$ as can be seen by approximating $\phi_V(t)$ with $\exp(-t/\tau)$ in the integral in Eq. (2). Figure 6 shows that the frequency dependent specific heat $C_V(\omega)$ versus ω increases with decreasing frequency and then flattens off when the period becomes longer than the inverse sampling time. This can be seen more clearly in Fig. 7 where we plot both the frequency dependent specific heat $C_V(\omega)$ versus the period as well as the specific heat versus the time span. Figure 7 shows that $C_V(\omega)$ continues to increase well beyond the α relaxation time and eventually saturates when the period is comparable to the minimum sampling time.

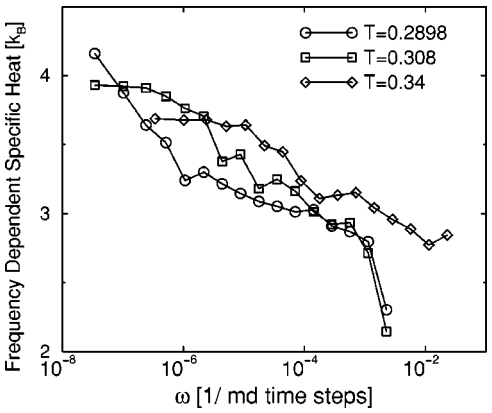

FIG. 6. Frequency dependent specific heat vs frequency for 512 particles at $T=0.289\,855$, $0.308\,642$, and $0.342\,4658$. Parameters are the same as in Fig. 2.

D. Absence of aging

We now cite evidence that systems at temperatures just below T_p have equilibrated in the sense of showing no signs of aging. First the inset of Fig. 2 shows the lack of aging in the specific heat versus time for a given value of Δt_b. Second is the absence of aging in the α relaxation time τ. As we

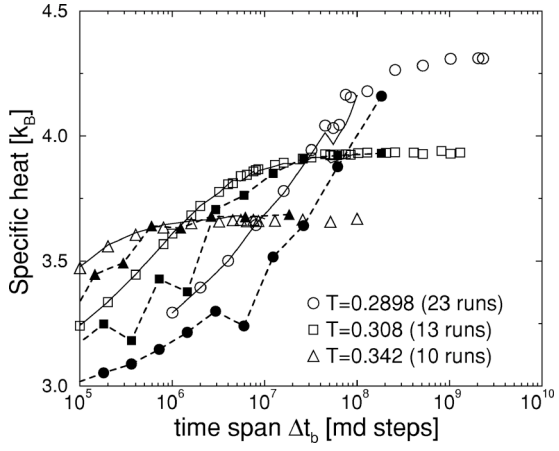

FIG. 7. Frequency dependent specific heat vs inverse frequency or the period in MD time steps for 512 particles. Also shown for comparison is the data from Fig. 2. The solid symbols with the dashed lines are $C_V(\omega)$ at three different temperatures. The shape of the symbols indicates the temperature as given in the legend.

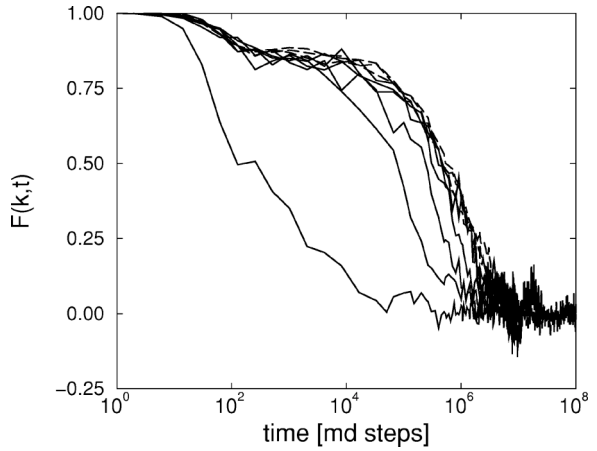

FIG. 8. Full intermediate scattering function $F_{BB}(k_{\max},t)$ vs time for 512 particles of which 256 are type B particles. $k_{\max}=2\pi \times 8.3666/L$. The solid lines come from averaging $F_{BB}(k_{\max},t)$ over 11 different runs, each of which was started from $T=1.5$, quenched to $T=0.289\,855$, and then used to calculate $F_{BB}(k_{\max},t)$ after a waiting time of t_W. From left to right, $t_W=0$, 5×10^4, 5×10^5, 10^6, 5×10^6, and 2.5×10^7 MD steps. The dashed lines correspond to averaging over 40 runs with $t_W=5\times10^7$, 10^8, and 1.5×10^8 time steps during single temperature runs at $T=0.289\,855$.

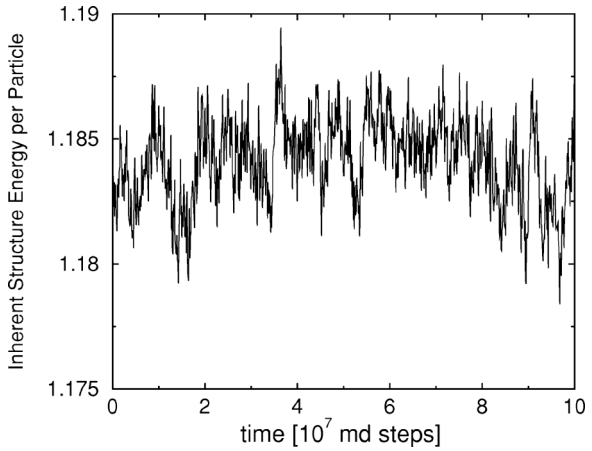

FIG. 9. Inherent structure energy per particle vs time for 512 particles at $T=0.289\,855$ averaged over 40 single temperature runs. Each run was started from a configuration generated from parallel tempering at $T=0.289\,855$, equilibrated for 5×10^7 time steps, and then run for an additional 1×10^8 time steps during which configurations were periodically recorded. The energies of the inherent structures associated with these recorded configurations are shown here. The inherent structure energy per particle is measured in MD units.

described earlier, we have calculated τ using the full intermediate scattering function $F_{BB}(\vec{k},t)$ for the B particles. The relaxation time τ is defined by $F(k,\tau)/F(k,t=0)=1/e$. We have averaged $F(k,t)/F(k,t=0)$ over 40 runs after waiting times t_W of 5×10^7, 10^8, and 1.5×10^8 time steps for a system with 512 particles at $T=0.289\,855<T_p$ [29]. We find that the α relaxation time $\tau=(1.0\pm0.1)\times10^6$ MD time steps. This value of τ shows no signs of aging [6] in the sense that there is no systematic variation with waiting time. The lack of aging is to be expected since the aging time is equal to τ which is much less than t_W. We have confirmed that the aging time is the same as the equilibrium value of τ by starting from 11 different equilibrium configurations at $T=1.5$, quenching to $T=0.289\,855$, and measuring τ after waiting times of $t_W=0$, 5×10^4, 5×10^5, 10^6, 5×10^6, and 2.5×10^7 MD steps. The results are shown in Fig. 8. For $t_W<10^6$ MD steps, τ increases with t_W which indicates aging [6]. However, for $t_W\geqslant10^6$ MD steps, there is no aging and τ equals its equilibrium value of 10^6 MD steps.

Third we have looked for signs of aging in the inherent structure energy versus time in our single temperature molecular dynamics runs of 10^8 time steps at $T=0.289\,855<T_p$. During the run, configurations were recorded every so often. Averaging over 40 runs, we find no evidence that the inherent structure energy decreases systematically with time, though the noise in the data prevents us from seeing changes smaller than 1%. This is shown in Fig. 9.

We have also examined the root mean square displacement $\langle\Delta r^2(t)\rangle^{1/2}$ in our long single temperature runs where

$$\langle\Delta r^2(t)\rangle=(1/N)\left\langle\sum_{i=1}^{N}[\mathbf{r}_i(t)-\mathbf{r}_i(0)]^2\right\rangle. \tag{3}$$

We found that $\langle\Delta r^2(t)\rangle^{1/2}\gtrsim10\sigma_A$ in each run examined after 10^8 time steps at $T=0.289\,855$. This is comparable to the box size $L=9.48\sigma_A$ for a system of 512 particles. So the system does not appear to be getting stuck in a metastable minimum of the energy landscape during the single temperature runs. Note that even though the root mean square displacement is comparable to the size of the system, the system still has not sampled enough configurations to obtain its thermodynamic value. Thus those who do simulations should be careful when their criterion for equilibration is that the root mean square displacement is a few particle diameters [44].

IV. DISCUSSION

As we mentioned in the Introduction, experiments find that in equilibrium systems at low frequencies the real part of the frequency dependent specific heat rises and then saturates with decreasing frequency [2,3,9–15]. There have been a number of theoretical approaches to describe the frequency dependent specific heat [16–25]. Some have viewed the frequency dependent specific heat in the context of generalized hydrodynamic equations [17,18]. Nielsen and Dyre derived the fluctuation-dissipation theorem for the frequency dependent specific heat [22]. Some have suggested that slow structural relaxation leads to slow thermal relaxation which results in a frequency dependent specific heat [18,23]. Zwanzig related $C_p(\omega)$ to the frequency dependent longitudinal viscosity [20]. His work implies that in isobaric measurements a

change in temperature produces a change in the density leading to a slow volume relaxation due to the high value of the viscosity [25]. Thus the frequency dependent viscosity produces a frequency dependent specific heat $C_p(\omega)$ at constant pressure. Zwanzig assumes that the constant volume specific heat is independent of frequency. However, our constant volume simulations as well as those of others [19,25] indicate that there must be a different reason for the frequency dependence of the specific heat. Simon and McKenna [16] suggested that the application of high frequency heat current oscillations drives the system out of equilibrium by putting the system in the vicinity of the frequency dependent T_g. They argue that as a result the response is dominated by structural recovery. However, we find a frequency dependent specific heat for a system that is in equilibrium, and shows no signs of aging or structural relaxation. We did not allow temperature oscillations. Rather we kept the temperature constant and used the energies of an equilibrium system to calculate $C_V(\omega)$.

To understand why the specific heat has frequency dependence at low frequencies, note that the increase and eventual saturation of the zero frequency specific heat with increasing time span is mirrored by the rise and subsequent saturation of the frequency dependent specific heat with decreasing frequency. Longer time spans correspond to longer periods and lower frequencies. Just as long time spans are needed to acquire a sufficient sampling of the energy to produce the equilibrium value of the specific heat, the period must be long enough for the energies to become uncorrelated in order for the frequency dependent specific heat to approach its zero frequency equilibrium value. To show this, we can make an estimate of the frequency dependent specific heat by roughly approximating the energy autocorrelation function in Eq. (2) with $\phi_V(t)=A\exp(-t/\tau_L)$ [45]. Doing the integral in Eq. (2) produces a Lorentzian:

$$C_V'(\omega) = C_{eq} - A\frac{\omega^2\tau_L^2}{1+\omega^2\tau_L^2}. \tag{4}$$

We will refer to this as the Debye model of the frequency dependent specific heat. Using a simple exponential to fit the energy autocorrelation function produced by averaging over 23 runs at $T=0.289\,85$ with intervals of 350 MD steps results in a rather poor fit, but produces the values $\tau_L=4\,825\,379$ time steps and $A=0.773k_B$. The result of using these values in Eq. (4) is shown in Fig. 10 as well as the result of setting τ_L equal to the α relaxation time $\tau_L=\tau=10^6$ MD steps. Note that the frequency dependent specific heat starts to rise when the period is comparable to τ_L, the energy correlation time. In other words in this simple model the frequency dependent specific heat starts to increase when the period is long enough for the energies to become uncorrelated and for the system to begin to sample independent energies.

In our simulations, comparing our energy correlation times to Fig. 6 indicates that as the frequency decreases, the rise in the frequency dependent specific heat begins at frequencies higher than the inverse energy correlation time. This is not surprising since the energy correlation function is better fit by a stretched exponential function than by a simple exponential. The stretched exponential implies that $C_V(\omega)$ will rise over a larger range of frequencies than if the energy correlation function decayed as a simple exponential. From Eqs. (2) and (4) we see that the rise occurs as the energies become uncorrelated. The time scale for this to occur is the energy correlation time. Since the energy correlation time is comparable to the α relaxation time, this is consistent with other simulations that found the specific heat increasing with decreasing frequency at frequencies corresponding to the time scales of the structural relaxation. Our work shows that structural relaxation is not involved in the rise of the frequency dependent specific heat in an equilibrium system. Rather the rise is the result of the system sampling uncorrelated statistically independent energy fluctuations. The time scales required for sampling independent energies increase with decreasing temperature due to the slow microscopic dynamics that also govern the structural relaxation of a glass forming liquid.

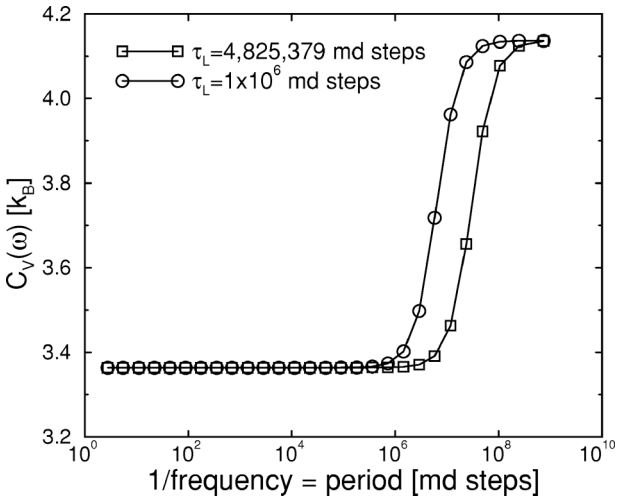

FIG. 10. Frequency dependent specific heat from Eq. (4) vs inverse frequency or the period in MD time steps at $T=0.289\,85$. In Eq. (4) we used $A=0.773k_B$ and $C_{eq}=4.136\,743k_B$.

The frequency dependent specific heat saturates when the period is long enough for the system to sample enough energies to obtain an accurate value for the equilibrium zero frequency specific heat, i.e., when the period reaches the minimum sampling time. This can be seen in Fig. 7 where we compare the frequency specific heat versus period to the specific heat versus time span. Both reach a plateau at about the same time, and this time is the minimum sampling time. Returning to our simple example of the Debye model, we can see from Fig. 10 that the minimum sampling time is almost two orders of magnitude larger than τ_L. For $\tau_L=4\,825\,379$ the minimum sampling time is about 2.5×10^8 MD steps, and for $\tau_L=10^6$ MD steps, the minimum sampling time is about 5×10^7 MD steps. The fact that Eq. (4) only involves τ_L and yet produces a much longer minimum sampling time shows that the minimum sampling time is not a new time scale but just a reflection of the energy correlation time, or equivalently, the α relaxation time τ.

Furthermore, both the minimum sampling time and τ have roughly the same temperature dependence. This is shown in

Fig. 4. The points for the minimum sampling time are rather rough because there is no unambiguous way to define the minimum sampling time. So we simply defined it to be the earliest time where the value of the specific heat reached the equilibrium value and estimated it from the plots of the specific heat versus time span. The fact that the minimum sampling time and τ have roughly the same temperature dependence is consistent with the minimum sampling time being a reflection of τ. According to the time-temperature superposition principle of mode coupling theory, any definition of the relaxation time in the vicinity of T_C that measures the time scale of the α relaxation is predicted to show the same temperature dependence [37].

Our work is a cautionary tale for those who perform numerical simulations on slowly relaxing systems. It indicates that to obtain accurate thermodynamic averages, one must not only check that the system shows no signs of aging, but one must also check that the quantity to be measured has sampled enough of phase space to obtain a large number of statistically independent values. This sampling time can be orders of magnitude longer than previously recognized time scales such as the aging time and the α relaxation time. Our method of calculating the specific heat as a function of the measurement time span is a systematic way of determining the equilibrium value. This method can be adapted for use in measuring other thermodynamic quantities. We believe it is an improvement over the sometimes arbitrary definitions of equilibration that have been invoked in doing numerical simulations.

Our approach for systematically calculating the equilibrium value of the specific heat is applicable for determining other thermodynamic quantities such as calculating the magnetic susceptibility from magnetization fluctuations, the dielectric constant from electric polarization fluctuations, and the conductivity from current fluctuations. In all these cases the thermodynamic average requires adequate sampling. Experimental measurements on glassy systems that show no signs of aging may also find that the results depend on the time span over which the measurements were made. If this is the case, the distribution of values will change with the amount of sampling time.

One should realize that different quantities can have different minimum sampling times even with fixed macroscopic parameters such as T, N, V, etc. We have seen that the time needed to determine the relaxation time can be orders of magnitude smaller than the time needed to find the equilibrium specific heat at $T<T_p$. One way to understand this is to consider the distribution of potential energies of the system. Finding the average energy will take less sampling than finding higher moments of the distribution such as the second moment which is reflected in the specific heat.

To summarize, experimental measurements on systems that are not aging have found that the specific heat is frequency dependent [2]. Our work shows that this frequency dependence arises from the long equilibration times needed to sample statistically independent energies, and that the specific heat becomes independent of frequency once the period exceeds the minimum sampling time.

ACKNOWLEDGMENT

We thank Francesco Sciortino, Bulbul Chakraborty, Jon Wellner, Greg McKenna and Sue Coppersmith for helpful discussions. This work was supported by U.S. Department of Energy Grant No. DE-FG03-00ER45843.

[1] M. D. Ediger, C. A. Angell, and S. R. Nagel, J. Phys. Chem. **100**, 13 200 (1996), and references therein.
[2] N. O. Birge and S. R. Nagel, Phys. Rev. Lett. **54**, 2674 (1985).
[3] P. K. Dixon *et al.*, Phys. Rev. Lett. **65**, 1108 (1990).
[4] M. Goldstein, J. Chem. Phys. **51**, 3728 (1969).
[5] S. Sastry, P. G. Debenedetti, and F. H. Stillinger, Nature (London) **393**, 554 (1998).
[6] W. Kob and J. L. Barrat, Phys. Rev. Lett. **78**, 4581 (1997).
[7] D. N. Perera and P. Harrowell, Phys. Rev. E **59**, 5721 (1999).
[8] I. Saika-Voivod, P. H. Poole, and F. Sciortino, Nature (London) **412**, 514 (2001).
[9] N. O. Birge, Phys. Rev. B **34**, 1631 (1986).
[10] P. K. Dixon and S. R. Nagel, Phys. Rev. Lett. **61**, 341 (1988).
[11] N. Menon, J. Chem. Phys. **105**, 5246 (1996).
[12] T. Christensen, J. Phys. (Paris), Colloq. **46**, 635 (1985).
[13] H. Leyser, A. Schulte, W. Doster, and W. Petry, Phys. Rev. E **51**, 5899 (1995).
[14] Y. H. Jeong and I. K. Moon, Phys. Rev. B **52**, 6381 (1995).
[15] M. Beiner *et al.*, Macromolecules **29**, 5183 (1996).
[16] S. L. Simon and G. B. McKenna, J. Chem. Phys. **107**, 8678 (1997).
[17] D. W. Oxtoby, J. Chem. Phys. **85**, 1549 (1986).
[18] J. Jäckle, Z. Phys. B: Condens. Matter **64**, 41 (1986).
[19] G. S. Grest and S. R. Nagel, J. Phys. Chem. **91**, 4916 (1987).
[20] R. Zwanzig, J. Chem. Phys. **88**, 5831 (1988).
[21] W. Götze and A. Latz, J. Phys.: Condens. Matter **1**, 4169 (1989).
[22] J. K. Nielsen and J. C. Dyre, Phys. Rev. B **54**, 15754 (1996).
[23] J. Jäckle, Physica A **162**, 377 (1990).
[24] J. K. Nielsen, Phys. Rev. E **60**, 471 (1999).
[25] P. Scheidler *et al.*, Phys. Rev. B **63**, 104204 (2001).
[26] T. A. Weber and F. H. Stillinger, Phys. Rev. B **31**, 1954 (1985).
[27] W. Kob and H. C. Andersen, Phys. Rev. Lett. **73**, 1376 (1994).
[28] W. Götze and L. Sjögren, Rep. Prog. Phys. **55**, 241 (1992).
[29] H. M. Carruzzo and C. C. Yu, Phys. Rev. E **66**, 021204 (2002).
[30] D. C. Rapaport, *The Art of Molecular Dynamics Simulation* (Cambridge University Press, New York, 1995).
[31] W. G. Hoover, A. J. C. Ladd, and B. Moran, Phys. Rev. Lett. **48**, 1818 (1982).
[32] D. J. Evans, J. Chem. Phys. **78**, 3297 (1983).
[33] D. J. Evans *et al.*, Phys. Rev. A **28**, 1016 (1983).
[34] D. J. Evans and G. P. Morriss, Comput. Phys. Rep. **1**, 297 (1984).
[35] W. Kob, C. Brangian, T. Stuhn, and R. Yamamoto, in *Com-*

puter Simulation Studies in Condensed Matter Physics XIII, edited by D. P. Landau, S. P. Lewis, and H. B. Schuttler (Springer-Verlag, Berlin, 2001), p. 153.

[36] A. Rinaldi, F. Sciortino, and P. Tartaglia, Phys. Rev. E **63**, 061210 (2001).

[37] W. Kob and H. C. Andersen, Phys. Rev. E **52**, 4134 (1995).

[38] We have also fit $F_{BB}(k_{\max},t)/F_{BB}(k_{\max},t=0)$ averaged over 40 runs at $T=0.289\,855$ to a stretched exponential form, i.e., $F_{BB}(k_{\max},t)/F_{BB}(k_{\max},t=0)=\exp[-(t/\tau)^{\lambda}]$. We find that $\lambda=0.62$ and $\tau=1.01\times10^{6}$ MD steps. Note that in this case τ has the same value as the α relaxation time.

[39] F. H. Stillinger and T. A. Weber, Phys. Rev. A **25**, 978 (1982).

[40] W. H. Press, S. A. Teukolsky, W. T. Vetterling, and B. P. Flannery, *Numerical Recipes in C: The Art of Scientific Computing* (2nd ed.) (Cambridge University Press, Cambridge, UK, 1992), p. 420.

[41] A. M. Ferrenberg, D. P. Landau, and K. Binder, J. Stat. Phys. **63**, 867 (1991).

[42] M. P. Allen and D. J. Tildesley, *Computer Simulations of Liquids* (Oxford University Press, Oxford, 1987).

[43] T. B. Schroder, S. Sastry, J. G. Dyre, and S. C. Glotzer, J. Chem. Phys. **112**, 9834 (2000).

[44] M. Hemmati, C. T. Moynihan, and C. A. Angell, J. Chem. Phys. **115**, 6663 (2001).

[45] A stretched exponential function would be a better approximation to the energy autocorrelation function, but it would not allow us to obtain an analytic expression for the frequency dependent specific heat from Eq. (2).